Inorganic Chemistry

Communication

pubs.acs.org/IC

A Highly Selective Fluorescent Chemosensor for Al^{III} Ion and Fluorescent Species Formed in the Solution

Wei-Hua Ding,[†] Wei, Cao,[†] Xiang-Jun Zheng,*[,†] De-Cai Fang,*[,†] Wing-Tak Wong,[‡] and Lin-Pei Jin[†]

[†]Beijing Key Laboratory of Energy Conversion and Storage Materials, College of Chemistry, Beijing Normal University, Beijing 100875, People's Republic of China

[‡]Department of Applied Biology & Chemical Technology, The Hong Kong Polytechnic University, Hung Hom, Hong Kong SAR, People's Republic of China

Supporting Information

ABSTRACT: A chemosensor for the Al^{3+} ion, 1-[(3-hydroxypyridin-2-ylamino)methylene]naphthalen-2(1*H*)-one (H_2L), based on inhibited excited-state intramolecular proton transfer was synthesized. The experimental and theoretical calculations at B3LYP+PCM/6-31G(d) revealed that Al^{3+} and H_2L form a 1:1 complex, $[AlL(OH)(H_2O)]_2$, in dimethyl sulfoxide that exhibits two remarkably enhanced fluorescent emissions at 523 and 553 nm. It is confirmed that H_2L could be used to detect Al^{3+} ions in cells by bioimaging.

As is known, the Al^{3+} ion existing in natural waters and most plants[1] can enter the human body through foods and water.[2] The average daily intake of Al^{3+} ions for the human body is about 3−10 mg/day.[3] Excess aluminum could induce health issues, for instance, Parkinson's disease.[4] Thus, the detection of Al^{3+} has attracted increasing interest in the areas of chemical and biological sciences. Compared with some conventional methods, fluorescent chemosensors have attracted significant focus because of their high sensitivity, simplicity, and real-time monitoring with rapid response time.[3,5,6] Recently, some fluorescent sensors for detection of the Al^{3+} ion have been reported.[5b,7] However, most of them require complicated syntheses involving harsh reaction conditions and expensive chemicals. Therefore, it is important to develop sensors with high selectivity and sensitivity for Al^{3+}, and it should be easily prepared and can be applied in cell bioimaging. As a chemosensor, a Schiff base is popular owing to its good photophysical properties;[8] Schiff base derivatives equipped with a fluorescence moiety are attractive tools for the detection of metal cations. Some Schiff base chemosensors for the Al^{3+} ion have been reported.[7c,h] Meanwhile, several sensing mechanisms of fluorescent chemosensors have been exploited. Among these mechanisms, excited-state intramolecular proton transfer (ESIPT)-based chemosensors are ideal candidates for fluorescence probes because of the almost complete lack of spectral overlap between absorption and emission.[9] The ESIPT process generally involves the transfer of a hydroxyl (or amino) proton to a neighboring carbonyl oxygen (or imine nitrogen) through a preexisting six- or five-membered ring of hydrogen-bonding configuration, which leads to very weak fluorescence or nonfluorescence.[9,10] If they are coordinated with metal ions, metal coordination will remove this proton and inhibit the ESIPT process, and a significant emission enhancement can be observed. Herein, we report a chemosensor for Al^{III} based on inhibition of ESIPT. The complex species formed in the solution and the two-band emission were inferred through experimental and theoretical methods. Furthermore, the chemosensor was used to detect the Al^{III} ion in cells by bioimaging.

2-Hydroxy-1-naphthaldehyde and 2-amino-3-hydroxypyridine were selected as the reactants to obtain the Schiff base. Single-crystal X-ray diffraction revealed that it forms a six-membered ring of intramolecular hydrogen bonding.[11] Also, it exists in the form of its isomer, a ketoamine form, 1-[(3-hydroxypyridin-2-ylamino)methylene]naphthalen-2(1*H*)-one (H_2L). It can change to its phenolimine form through intramolecular proton transfer, as shown in Scheme 1.[12] Its crystal structure is similar to

Scheme 1. Structures of Keto and Enol Forms of H_2L

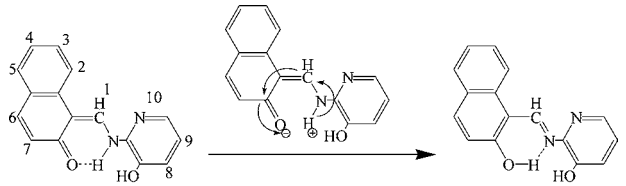

that reported.[13] H_2L in dimethyl sulfoxide (DMSO) displays very weak fluorescence with a low quantum yield (Φ = 0.007) when excited at 466 nm. Then, the selectivity of H_2L to various metal ions was examined in DMSO. In the emission spectra, as shown in Figure 1, the addition of 1.0 equiv of Na^+, K^+, Mg^{2+}, Ca^{2+}, Mn^{2+}, Fe^{3+}, Co^{2+}, Cr^{3+}, Cd^{2+}, Cu^{2+}, Pb^{2+}, Ni^{2+}, and Zn^{2+} had no effect on the fluorescence. However, upon the addition of 1.0 equiv of Al^{3+}, the fluorescence intensity of dual emission bands at 523 and 553 nm with a high quantum yield (Φ = 0.425) was largely enhanced. The fluorescence lifetime for the Al^{III} complex with H_2L in DMSO was measured from the decay profile (Figure S1 in the Supporting Information, SI) to obtain τ = 3.50 ± 0.01 ns. When the solutions of H_2L with various metal ions were excited at 365 nm, only the one with Al^{3+} showed strong yellow fluorescence that could be easily observed by the naked eye (Figure S2 in the SI).

Received: April 24, 2013
Published: June 20, 2013

   dx.doi.org/10.1021/ic401028u | *Inorg. Chem.* 2013, 52, 7320−7322

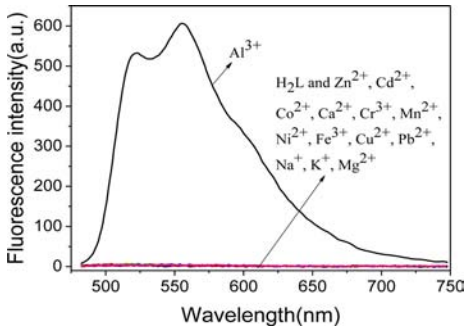

Figure 1. Fluorescence responses of H_2L (5 μM) in DMSO with 1.0 equiv of other metal ions. λ_{ex} = 466 nm.

To validate the high selectivity of H_2L for detection of Al^{3+} in practice, competitive fluorescence titration was carried out. H_2L was treated with 1.0 equiv of Al^{3+} in the presence of 1.0 equiv of other metal ions. There is no interference for the detection of Al^{3+} in the presence of all other metal ions (Figure S3 in the SI). A relatively low but clearly detectable fluorescence was observed in the presence of Cu^{2+} and Fe^{3+}. These results demonstrate that H_2L is highly selective for Al^{3+} in a DMSO solution.

To investigate the complexation of H_2L with Al^{3+} in DMSO, a Job plot based on fluorescence was operated. As shown in Figure S4 in the SI, a 1:1 stoichiometric complexation between H_2L and Al^{3+} was confirmed. In the fluorescence titration profiles, the intensity increases remarkably at 523 and 553 nm upon addition of the Al^{3+} ion until 1.0 equiv, and upon a further increase of the Al^{3+} concentration, the intensity tends to be the same (Figure S5 in the SI). To further know the detailed complexation of Al^{3+} with H_2L, ^1H NMR spectra of H_2L upon the addition of different concentrations of Al^{3+} in DMSO-d_6 were recorded. The label of H is shown in Scheme 1a. As shown in Figure 2a, the proton of C-

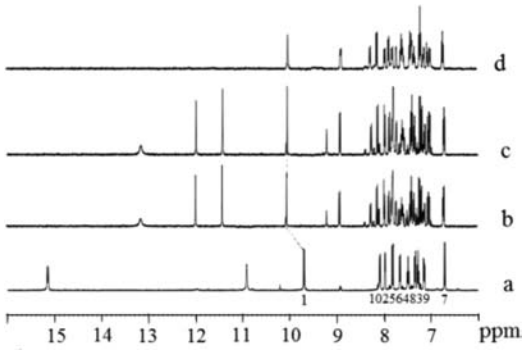

Figure 2. ^1H NMR spectra in DMSO-d_6: (a) H_2L only; (b) H_2L and 1.0 equiv of Al^{3+}; (c) H_2L and 1.5 equiv of Al^{3+}; (d) a drop of D_2O added to part b.

NH locating at >15 ppm is characteristic of an intramolecular hydrogen bond (Figure 2a).[14] Besides, both protons of C-NH and CH-N (H_1) exhibited doublets because of their intercoupling. Upon the addition of 1.0 equiv of Al^{3+}, the proton signals of −C-NH at 15.14 ppm and pyridine hydroxyl at 10.87 ppm disappeared (Figure 2b). The proton peak (H_1) of CH═N at 9.70 ppm was downfield shifted to a singlet at 10.05 ppm, and the protons (H_{2-10}) of naphthalene and pyridine at 6.70−8.10 ppm also experienced a downfield shift to 6.80−8.25 ppm upon complexation of Al^{3+} and H_2L.[12a] Compared to Figure 2b, there were no significant changes with the proton peaks upon the addition of 1.5 equiv of Al^{3+} to H_2L (Figure 2c). These results suggest that H_2L is coordinated to Al^{3+} by imine, naphthol hydroxyl, and pyridine hydroxyl, and the inhibition of ESIPT happens in a tridentate fashion for binding of Al^{3+}. In fact, even the small amount of moisture introduced with hydrated aluminum salts may suffice to hydrolyze and form hydroxylated aluminum compounds.[15] Besides, OH^- and H_2O can supply a hard-base environment for the hard-acid Al^{3+}, which makes it easier to form the Al^{III} complex.[16] Comparing parts b and d of Figure 2, one can find that signals at 11.98 and 11.42 ppm in Figure 2b disappeared in Figure 2d, showing possible coordination of the OH^- group and H_2O to the Al^{3+} ion. Also in the literature, a number of six-coordinated Al^{3+} complexes with μ-OH and H_2O could be found.[17] Furthermore, electrospray ionization mass spectrometry (ESI-MS) also indicates the 1:1 binding stoichiometry of H_2L with Al^{3+}. Upon the addition of 1.0 equiv of Al^{3+} to H_2L, the mass spectrum (Figure S6 in the SI) exhibited an intense peak at m/z 289.1 and a weak one at m/z 307.1, corresponding to the ion $[AlL]^+$ (calcd m/z 289.3) and $[AlLH_2O]^+$ (calcd m/z 307.2), respectively, and the peak at m/z 687.3 can be ascribed to $K^+[AlL(OH)(H_2O)]_2$ (calcd m/z 687.5). From the results of fluorescence titration, the Job plot, ESI-MS, and ^{1}HNMR data, the species formed in the solution can be considered as $[AlL(OH)(H_2O)]_2$.

To better understand the sensing mechanism and the structure−property relationship of the $[AlL(OH)(H_2O)]_2$ dimer, theoretical calculations, at the B3LYP+PCM/6-31G(d) level with DMSO as the solvent, were carried out. The obtained results showed that the hydrogen-transfer process for H_2L in ground and excited states results in two possible isomers, i.e., a and b (Figure S7 and Table S1 in the SI). In the ground state, H_2L is mainly in the keto form in equilibrium because the keto isomer is about 4.3 kcal/mol lower than that of the enol form. The hydrogen-transfer process from a to b needs to overcome an energy barrier of 6.4 kcal/mol, but its reverse process is only 2.1 kcal/mol. However, in the excited state of H_2L, such species with high energy will lead to the hydrogen-transfer process taking place more easily, which might result in very weak fluorescence for H_2L when excited. The cis/trans isomerization is not responsible for the loss of fluorescence because two factors will prevent rotation along the C═N bond: one is the hydrogen bond of N−H···O, and the other is the steric repulsion between two terminal groups. Upon coordination with Al^{3+}, the ESIPT process in H_2L is inhibited, resulting in large fluorescence enhancement.

Furthermore, the ground- and excited-state geometries as well as excited-state properties of the species $[AlL(OH)(H_2O)]_2$ dimer have been determined with theoretical calculations. The main geometric parameters for the ground and excited states are depicted (Figure S8 in the SI), from which one can observe that each Al^{3+} displays a six-coordination with one Al←N bond and five Al←O bonds. There is one C═N π bond connected to each Al←N bond, which is related to the molecular excitations. In the first excited state, only one of the C═N bonds in two ligands is lengthened about 0.061 Å, while the corresponding Al←N bond length is shortened with 0.091 Å. From the obtained ground-state geometry, the excitation energies (λ_{max}) and their corresponding oscillator strengths (F) can be calculated. In order to understand the excitations, the four frontier orbitals are depicted in Figure 3, from which one can observe that all of four frontier orbitals are mainly on a skeleton of ligands. LUMO and LUMO+1 orbitals are mainly C═N π^* orbitals but in different phases for two pieces of ligands. Because HOMO → LUMO is not symmetrically allowed, only HOMO → LUMO+1 and

dx.doi.org/10.1021/ic401028u | Inorg. Chem. 2013, 52, 7320−7322

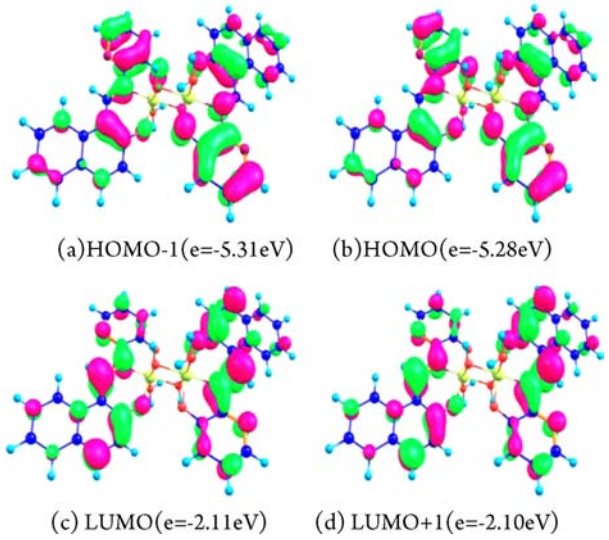

Figure 3. Frontier orbitals and their orbital energies for $[AlL(OH)(H_2O)]_2$.

HOMO−1 → LUMO excitations are calculated (Figure S8 in the SI), and their corresponding excitation energies are calculated as 442 and 440 nm, respectively. These two closer excitations will generate two fluorescence peaks of 525 and 568 nm (Figure S9 in the SI), with oscillator strengths being 0.30 and 0.70, which are in good agreement with two band emissions of 523 and 553 nm observed in our experiments. We also performed calculations for the monomer $[AlL(OH)(H_2O)]$, but only one band emission was found because there is only one C═N π bond in the ligand L instead of two C═N π bonds in $[AlL(OH)(H_2O)]_2$.

Having investigated the selectivity and sensitivity of H_2L toward the Al^{3+} ion, we further observed its potential application in cell imaging. For this purpose, the human cervical HeLa cancer cells were first incubated with $Al(NO_3)_3$ for 4 h and then treated with 10 μM H_2L for 30 min before imaging. As shown in Figure S10 in the SI, these cells that were not incubated with H_2L previously showed no fluorescence; in contrast, strong fluorescence was observed in cells exposed to H_2L. These results demonstrated that the chemosensor was membrane-permeable and could signal the presence of intracellular Al^{3+}.

In conclusion, a turn-on two-band fluorescence chemosensor for the Al^{3+} ion based on inhibition of the ESIPT process was obtained. Theoretical calculations explained the two-band emission phenomenon and revealed that neighboring −C═N and −C-OH groups or −C-NH and −C═O groups forming a six-membered ring of hydrogen bonding is essential for the ESIPT process of Schiff-base receptors.

■ ASSOCIATED CONTENT

Ⓢ Supporting Information

X-ray crystallographic data in CIF format, materials and methods, synthesis and characterization for H_2L, determination of the quantum yield, calculation methods, methods for cell imaging, Figures S1−S10, and Table S1. This material is available free of charge via the Internet at http://pubs.acs.org.

■ AUTHOR INFORMATION

Corresponding Author

*E-mail: xjzheng@bnu.edu.cn (X.-J.Z.), dcfang@bnu.edu.cn (D.-C.F.).

Notes

The authors declare no competing financial interest.

■ ACKNOWLEDGMENTS

This work is supported by the National Natural Science Foundation of China (Grant 20971015) and the Fundamental Research Funds for the Central Universities.

■ REFERENCES

(1) Park, H. M.; Oh, B. N.; Kim, J. H.; Qiong, W.; Jung, K. D.; Kim, C. *Tetrahedron Lett.* **2011**, *52*, 5581.

(2) (a) Burwen, D. R.; Olsen, S. M.; Bland, L. A.; Arduino, M. J.; Reid, M. H.; Jarvis, W. R. *Kidney Int.* **1995**, *48*, 469. (b) Berthon, G. *Coord. Chem. Rev.* **2002**, *228*, 319. (c) Yousef, M. I.; EI-Morsy, A. M. A.; Hassan, M. S. *Toxicology* **2005**, *215*, 97. (d) Bielarczyk, H.; Jankowska, A.; Madziar, B.; Matecki, A.; Michno, A.; Szutowicz, A. *Neurochem. Int.* **2003**, *42*, 323.

(3) (a) Barceló, J.; Poschenrieder, C. *Environ. Exp. Bot.* **2002**, *48*, 75. (b) Valeur, B.; Leray, I. *Coord. Chem. Rev.* **2000**, *205*, 3. (c) Rogers, M. A. M.; Simon, D. G. *Age Ageing* **1999**, *28*, 205. (d) Krejpcio, Z.; Wojciak, R. W. *Pol. J. Environ. Stud.* **2002**, *11*, 251.

(4) Altschuler, E. *Med. Hypotheses* **1999**, *53*, 22.

(5) (a) Zhu, J. W.; Qin, Y.; Zhang, Y. H. *Anal. Chem.* **2010**, *82*, 436. (b) Han, T. Y.; Feng, X.; Tong, B.; Shi, J. B.; Chen, L.; Zhi, J. G.; Dong, Y. P. *Chem. Commun.* **2012**, *48*, 416.

(6) Anbu, S.; Shanmugaraju, S.; Ravishankaran, R.; Karande, A. A.; Mukherjee, P. S. *Dalton Trans.* **2012**, *41*, 13330.

(7) (a) Arduini, M.; Tecilla, P. *Chem. Commun.* **2003**, 1606. (b) Kim, J. S.; Vicens, J. *Chem. Commun.* **2009**, *45*, 4791. (c) Kim, S.; Noh, J. Y.; Kim, K. Y.; Kim, J. H.; Kang, H. K.; Nam, S. W.; Kim, S. H.; Park, S.; Kim, C.; Kim, J. *Inorg. Chem.* **2012**, *51*, 3597. (d) Hau, F. K.; He, X. M.; Lam, W. H.; Yam, V. W. *Chem. Commun.* **2011**, *47*, 8778. (e) Lu, Y.; Huang, S. S.; Liu, Y. Y.; He, S.; Zhao, L. C.; Zeng, X. S. *Org. Lett.* **2011**, *13*, 5274. (f) Maity, D.; Govindaraju, T. *Chem. Commun.* **2010**, *46*, 4499. (g) Dong, Y.; Li, J. F.; Jiang, X. X.; Song, F. Y.; Cheng, Y. X.; Zhu, C. J. *Org. Lett.* **2011**, *13*, 2252. (h) Sahana, A.; Banerjee, A.; Lohar, S.; Sarkar, B.; Mukhopadhyay, S. K. *Inorg. Chem.* **2013**, *52*, 3627.

(8) (a) Silveira, V. C. D.; Luz, J. S.; Oliveira, C. C.; Graziani, I.; Ciriolo, M. R.; Ferreira, A. M. D. C. *J. Inorg. Biochem.* **2008**, *102*, 1090. (b) Padhyé, S.; Kauffman, G. B. *Coord. Chem. Rev.* **1985**, *63*, 127.

(9) (a) Wu, J. S.; Liu, W. M.; Ge, J. C.; Zhang, H. Y.; Wang, P. F. *Chem. Soc. Rev.* **2011**, *40*, 3483. (b) Henary, M. M.; Fahrni, C. J. *J. Phys. Chem. A* **2002**, *106*, 5210.

(10) Liu, Z. P.; He, W. J.; Guo, Z. J. *Chem. Soc. Rev.* **2013**, *42*, 1568.

(11) Crystal data for H_2L: $C_{16}H_{12}N_2O_2$, M_r = 264.26, monoclinic, space group $P2_1$, a = 8.7918(19) Å, b = 5.9020(13) Å, c = 12.126(3) Å, β = 90.288(4)°, V = 629.2(2) Å^3, Z = 2, D_c = 1.395 g/cm^3, μ = 0.094 mm^{-1}, $F(000)$ = 276, R1 = 0.0387, and wR2 = 0.0908.

(12) (a) Lin, H. Y.; Cheng, P. Y.; Wan, C. Y.; Wu, A. T. *Analyst* **2012**, *137*, 4415. (b) Fita, P.; Luzina, E.; Dziembowska, T.; Kopec, D.; Piatkowski, P.; Radzewicz, C.; Grabowska, A. *Chem. Phys. Lett.* **2005**, *416*, 305−310. (c) Zhang, X.; Guo, L.; Wu, F. Y.; Jiang, Y. B. *Org. Lett.* **2003**, *5*, 2667−2670.

(13) Ozek, A.; Yuce, S.; Albayrak, C.; Odabasoglu, M.; Buyukgungor, O. *Acta Crystallogr., Sect. E* **2004**, *60*, 356.

(14) Najafpour, M. M.; Tabrizi, M. A.; Haghighi, B.; Govindjee. *Dalton Trans.* **2013**, *42*, 879.

(15) Stavitski, E.; Goesten, M.; Juan-Alcaçiz, J.; Martinez-Joaristi, A.; Serra-Crespo, P.; Petukhov, A. V.; Gascon, J.; Kapteijn, F. *Angew. Chem., Int. Ed.* **2011**, *50*, 9624.

(16) Maity, D.; Govindaraju, T. *Inorg. Chem.* **2010**, *49*, 7229.

(17) (a) Wang, W.; Wentz, K. M.; Hayes, S. E.; Johnson, D. W.; Keszler, D. A. *Inorg. Chem.* **2011**, *50*, 4683. (b) Reinsch, H.; Marszalek, B.; Wack, J.; Senker, J.; Gil, B.; Stock, N. *Chem. Commun.* **2012**, *48*, 9486. (c) Reinsch, H.; Krüger, M.; Marrot, J.; Stock., N. *Inorg. Chem.* **2013**, *52*, 1854. (d) Reinsch, H.; van der Veen, M. A.; Marszalek, B.; Verbiest, T.; de Vos, D.; Stock, N. *Chem. Mater.* **2013**, *25*, 17. (e) Biswas, S.; Ahnfeldt, T.; Stock, N. *Inorg. Chem.* **2011**, *50*, 9518.